

Influence of cationic lipid composition on uptake and intracellular processing of lipid nanoparticle formulations of siRNA

Paulo J.C. Lin, PhD^{a,*}, Yuen Yi C. Tam, PhD^a, Ismail Hafez, PhD^a, Ammen Sandhu, PhD^b, Sam Chen, BSc^a, Marco A. Ciufolini, PhD^c, Ivan R. Nabi, PhD^d, Pieter R. Cullis, PhD^a

^aDepartment of Biochemistry and Molecular Biology, University of British Columbia, Vancouver, British Columbia, Canada

^bTekmira Pharmaceuticals Corporation, Burnaby, British Columbia, Canada

^cDepartment of Chemistry, University of British Columbia, Vancouver, British Columbia, Canada

^dDepartment of Cellular and Physiological Sciences, University of British Columbia, Vancouver, British Columbia, Canada

Received 8 November 2011; accepted 29 May 2012

Abstract

The *in vivo* gene silencing potencies of lipid nanoparticle (LNP)-siRNA systems containing the ionizable cationic lipids DLinDAP, DLinDMA, DLinKDMA, or DLinKC2-DMA can differ by three orders of magnitude. In this study, we examine the uptake and intracellular processing of LNP-siRNA systems containing these cationic lipids in a macrophage cell-line in an attempt to understand the reasons for different potencies. Although uptake of LNP is not dramatically influenced by cationic lipid composition, subsequent processing events can be strongly dependent on cationic lipid species. In particular, the low potency of LNP containing DLinDAP can be attributed to hydrolysis by endogenous lipases following uptake. LNP containing DLinKC2-DMA, DLinKDMA, or DLinDMA, which lack ester linkages, are not vulnerable to lipase digestion and facilitate much more potent gene silencing. The superior potency of DLinKC2-DMA compared with DLinKDMA or DLinDMA can be attributed to higher uptake and improved ability to stimulate siRNA release from endosomes subsequent to uptake.

From the Clinical Editor: This study reports on the *in vivo* gene silencing potency of lipid nanoparticle-siRNA systems containing ionizable cationic lipids. It is concluded that the superior potency of DLinKC2-DMA compared with DLinKDMA or DLinDMA can be attributed to their higher uptake thus improved ability to stimulate siRNA release from endosome.

© 2013 Elsevier Inc. All rights reserved.

Key words: Lipid nanoparticle; siRNA delivery; Biodegradability

The ability of small interfering double stranded RNA (siRNA) oligonucleotides to silence specific genes has significant potential for the development of new therapeutics. Sophisticated delivery technologies are required to realize this potential, however, because “naked” siRNA molecules are rapidly broken down in biologic fluids, are rapidly cleared from the circulation, do not accumulate at disease sites and cannot penetrate target cell membranes to reach their intracellular site of action. As a result, considerable efforts have been made to develop appropriate delivery vehicles.^{1,2}

P.R.C. has a financial interest in Tekmira Pharmaceuticals and receives grant funding from Alnylam Pharmaceuticals. No conflict of interest was reported by the other authors for this report.

Supported by Canadian Institutes for Health Research (CIHR) under University-Industry grant FRN59836, Tekmira Pharmaceuticals and Alnylam Pharmaceuticals.

*Corresponding author: Department of Biochemistry and Molecular Biology, University of British Columbia, Vancouver, British Columbia, Canada V6T 1Z3.

E-mail address: PauloL@mail.ubc.ca (P.J.C. Lin).

Lipid nanoparticles (LNP) represent the most clinically advanced systemic drug delivery system available with six LNP drugs having received regulatory approval for delivery of conventional “small molecule” pharmaceuticals.³ Significant progress has also been made toward developing LNP systems for nucleic acid-based drugs such as immunostimulatory oligonucleotides,^{4,5} plasmid DNA containing therapeutic genes,^{6,7} and antisense oligonucleotides.^{8,9}

LNP systems are also of increasing utility for the *in vivo* delivery of siRNA.^{10,11} The most promising LNP-siRNA systems contain ionizable cationic lipids with pKa values below 7 that allow the LNP to exhibit little positive charge at physiological pH.¹² LNP with low surface charge exhibit reduced toxicity as compared with charged systems, and enable long circulation lifetimes following intravenous (iv) injection, resulting in access to tissues other than the liver.^{8,9} Recent work¹² has shown that the *in vivo* gene silencing potency of these LNP-siRNA systems for hepatocyte targets is sensitive to relatively small molecular differences in the ionizable cationic lipid. Specifically, it was found that for LNP systems containing 1,2-dilinoleoyl-3-dimethylaminopropane

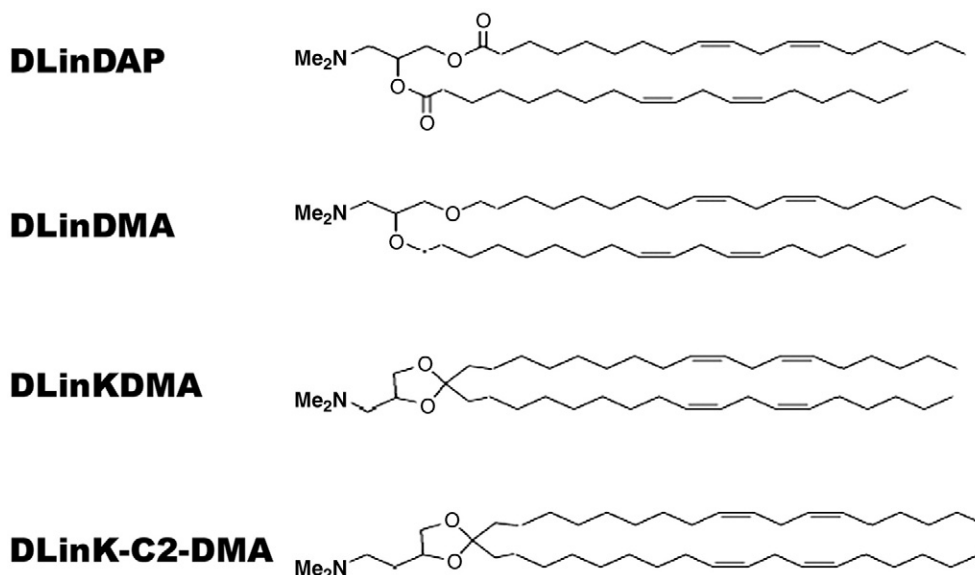


Figure 1. Ionizable cationic lipids.

(DLinDAP), 1,2-dilinolexyloxy-3-dimethylaminopropane (DLinDMA), 2,2-dilinoleyl-4-dimethylaminomethyl-[1,3]-dioxolane (DLinKDMA), or 2,2-dilinoleyl-4-(2-dimethylaminoethyl)-[1,3]-dioxolane (DLinKC2-DMA) (Figure 1) the *in vivo* activity varied over three orders of magnitude according to DLinKC2-DMA > DLinKDMA > DLinDMA >> DLinDAP. Similar potency trends have been observed in *in vivo* gene silencing studies in prostate tumor tissue¹³ and antigen-presenting cells (APC) of the immune system.¹⁴ LNP systems, like other foreign particles, are largely cleared from the blood by the fixed and free macrophages and dendritic cells of the reticuloendothelial system,^{15,16} leading to potentially efficient delivery of genetic material to modulate APC function. Potential target genes in APCs include inhibition of TNF α for alleviating inflammatory disease^{17–19} to modulation of CD40, CD80, and CD86, which are implicated in rheumatoid arthritis^{20–22} and act on costimulatory pathways in transplant rejection.^{23–25}

To improve current LNP systems for gene silencing, it is necessary to understand the mechanisms whereby one species of cationic lipid could give rise to superior gene silencing capabilities as compared with another, we investigate in this study the uptake, siRNA distribution and intracellular processing, and gene silencing activities of LNP containing DLinKC2-DMA, DLinKDMA, DLinDMA, and DLinDAP using a macrophage cell line. It is shown that the relative potency of the LNP systems correlates with uptake, intracellular processing, and cytoplasmic delivery of LNP contents. The sensitivity of cationic lipid to degradation by endogenous lipases following uptake can have particularly marked effects on gene silencing potency.

Methods

Formulation of LNP-siRNA systems

DLinDAP, DLinDMA, DLinKDMA, DLinKC2-DMA, and PEG-s-DMG were either obtained from Tekmira Pharmaceuticals

or Alnylam Pharmaceuticals or synthesized according to established methods. DSPC and cholesterol were obtained from Avanti (Alabaster, Alabama) and Sigma-Aldrich Co (St. Louis, Missouri). Lipophilic carbocyanine dyes to monitor LNP-siRNA uptake SPDIOC₁₈ (3,3'-dioctadecyl-5,5'-di[4-sulfophenyl] oxacarbocyanine) and DiIC₁₈ (1,1'-dioctadecyl-3,3,3',3'-tetramethylindocarbocyanine perchlorate) were obtained from Invitrogen (Carlsbad, California). All lipid stocks were dissolved and maintained in 100% ethanol. Lipids were mixed together at a molar % ratio of 40% cationic lipid, 2.5% PEG-s-DMG, 39.8% cholesterol, 17.5% DSPC, and 0.2% SPDIOC₁₈ or DiIC₁₈. The lipid mixture was added drop-wise to the formulation buffer (50 mM acetate, pH 4.0) to form multilamellar vesicles (MLV), which were processed to large unilamellar vesicles (LUVs) by extrusion through two stacked 80 nm Nuclepore polycarbonate filters using an Extruder (Northern Lipids, Vancouver, British Columbia, Canada) at ~300 psi. The preformed vesicles in 30% ethanol/70% 50 mM acetate, pH 4.0 were used for siRNA encapsulation.

Encapsulation of siRNA was achieved by drop-wise addition of the siRNA solution at 2.35 mg/mL in 30% ethanol/70% 50 mM acetate, pH 4.0 to preformed vesicles and incubated at 31°C for 30 minutes with constant stirring, followed by dialysis in PBS for 16 hours to remove the ethanol and neutralize the buffer. LNP size was determined by dynamic light scattering using a NICOMP370 particle sizer (Nicomp Particle Sizing Inc, Santa Barbara, California). Encapsulation efficiency was determined by quantifying siRNA by measuring absorbance at 260 nm in samples collected before and after dialysis following removal of free siRNA using VivaPureD MiniH columns (Sartorius Stedim Biotech, Aubagne, France). Lipid concentration was determined by measurement of cholesterol content by using a Cholesterol E enzymatic assay (Wako Chemicals USA, Richmond, Virginia).

Cell and reagents

Raw 264.7 cells were maintained in DMEM (Invitrogen) supplemented with 10% FBS at 37°C/5% CO₂. Cy3-siRNAs

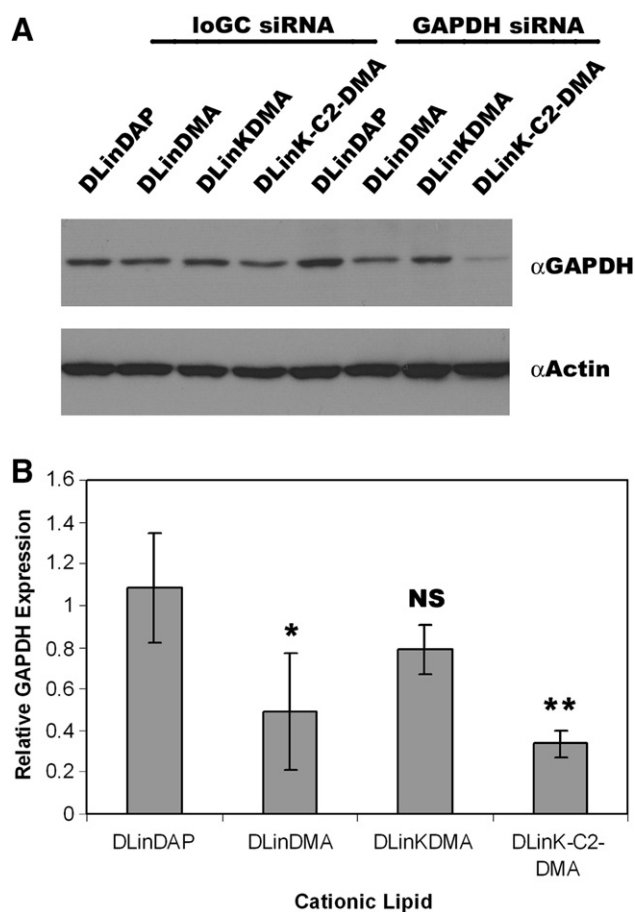


Figure 2. LNP-siRNA systems containing DLinKC2-DMA exhibit improved gene silencing in vitro as compared with other ionizable cationic lipids. **(A)** GAPDH siRNA or loGC siRNA (negative control siRNA) was formulated into LNP systems containing DLinDAP, DLinDMA, DLinKDMA, or DLinKC2-DMA in the molar ratios cationic lipid/DSPC/cholesterol/PEG-lipid 40/17.5/40/2.5. Raw 264.7 cells (9.5×10^4) were incubated with LNP-siRNA (1 mL; 10 $\mu\text{g}/\text{mL}$ or 700 nM of siRNA) for 72 h. GAPDH protein expression was assessed by Western blotting. **(B)** Relative GAPDH expression was measured from three independent experiments; \pm values indicate standard deviations. ANOVA analysis/Tukey-Kramer Multiple comparisons test was performed. DLinDAP versus DLinDMA $*P < 0.05$, DLinDAP versus DLinKDMA NS (not significant), DLinDAP versus DLinKC2-DMA $**P < 0.01$.

(sequence AD1991 and AD18560) were kindly provided by Alnylam Pharmaceuticals (Boston, Massachusetts)¹⁰ and glyceraldehyde 3-phosphate dehydrogenase (GAPDH) siRNA (sense strand 5'-UGGCCAAGGUCAUCAUGAdTdT-3' and antisense strand 5'-UCAUGGAUGCCUUGGCCAdTdT-3')²⁶ was purchased from Thermo Scientific (Waltham, Massachusetts). LoGC siRNA (negative control siRNA), Alexa 594-conjugated Transferrin, and Alexa 488-conjugated Escherichia coli BioParticles were purchased from Invitrogen. Rabbit polyclonal anti-GAPDH and anti-actin antibodies were purchased from Abcam (Cambridge, Massachusetts), and HRP-conjugated goat anti-rabbit IgG was purchased from Jackson ImmunoResearch Laboratories (West Grove, Pennsylvania). Porcine pancreatic lipase, genistein, nystatin, chlorpromazine, and amiloride were purchased from Sigma-Aldrich Co.

Table 1
LNP-siRNA properties

LNP-siRNA	Size (nm)	SD	Measured siRNA/lipid (wt/wt)
DLinDAP	85.4	20.9	0.085
DLinDMA	80.7	17.3	0.087
DLinKDMA	82.5	26.6	0.086
DLinKC2-DMA	75.2	29.3	0.091

Gene silencing

Raw 264.7 cells (9.5×10^4) were treated with 1 mL of 10 $\mu\text{g}/\text{mL}$ (~700 nM) GAPDH siRNA or loGC siRNA encapsulated in LNPs (LNP-siRNA) for 72 hours in complete growth media. Protein was extracted with lysis buffer (0.5% deoxycholic acid, 1.0% Igepal CA630 in $1 \times$ PBS, pH 7.4) supplemented with protease inhibitors for 30 minutes on ice. Protein (2.5 μg) was immunoblotted with 1° anti-GAPDH or α -actin rabbit polyclonal, and goat anti-rabbit HRP-conjugated 2° antibodies, followed by detection with Millipore Immobilon Western Chemiluminescent HRP substrate (Billerica, Massachusetts).

Fluorescence microscopy

Raw 264.7 cells (2×10^5) were grown on glass coverslips overnight and then treated with 1 mL of 10 μg siRNA/mL (700 nM) LNP Cy3-siRNA. The uptake of LNPs was monitored using SPDiO and overall distribution of siRNA was monitored using Cy3-labelled siRNA. Cells were fixed with 3% paraformaldehyde in PBS in the presence of Hoechst stain (Invitrogen) for nuclear staining for 15 minutes. Glass coverslips were mounted onto slides and analyzed by confocal microscopy (Olympus FV1000). Fluorochromes were excited at 405 nm (Hoechst stain), 488 nm (DiO), and 550 nm (Cy3 or DiI) and images were collected sequentially with 60 \times oil immersion objective lens.

LNP uptake

Raw 264.7 cells (1×10^4) were seeded and treated with 100 μL of 10 μg siRNA/mL (700 nM) of LNP Cy3-siRNA for 24 hours. Cells were fixed with 3% paraformaldehyde in PBS in the presence of Hoechst stain for 15 minutes. Cells were rinsed and stored in PBS supplemented with calcium chloride and magnesium sulfate. Plates were scanned and analyzed with the Cellomics ArrayScan VTI (Thermo Scientific) and the average intensity of Cy3 and DiO were measured.

Acid inhibition of clathrin mediated endocytosis

Raw 264.7 (2×10^5) cells were rinsed and incubated with DMEM supplemented with 10 mM HEPES pH 5.0 for 30 minutes at 37°C/5% CO₂. Cells were then rinsed with DMEM (10 mM HEPES and 10 mM acetic acid pH 5.0) for 10 minutes at 37°C/5% CO₂ and incubated with 1 mL of 10 μg siRNA/mL (700 nM) of LNP Cy3-siRNA or 1 $\mu\text{g}/\text{mL}$ of Alexa 594-conjugated Transferrin in DMEM (10 mM HEPES and 10 mM acetic acid pH 5.0) for 6 hours.

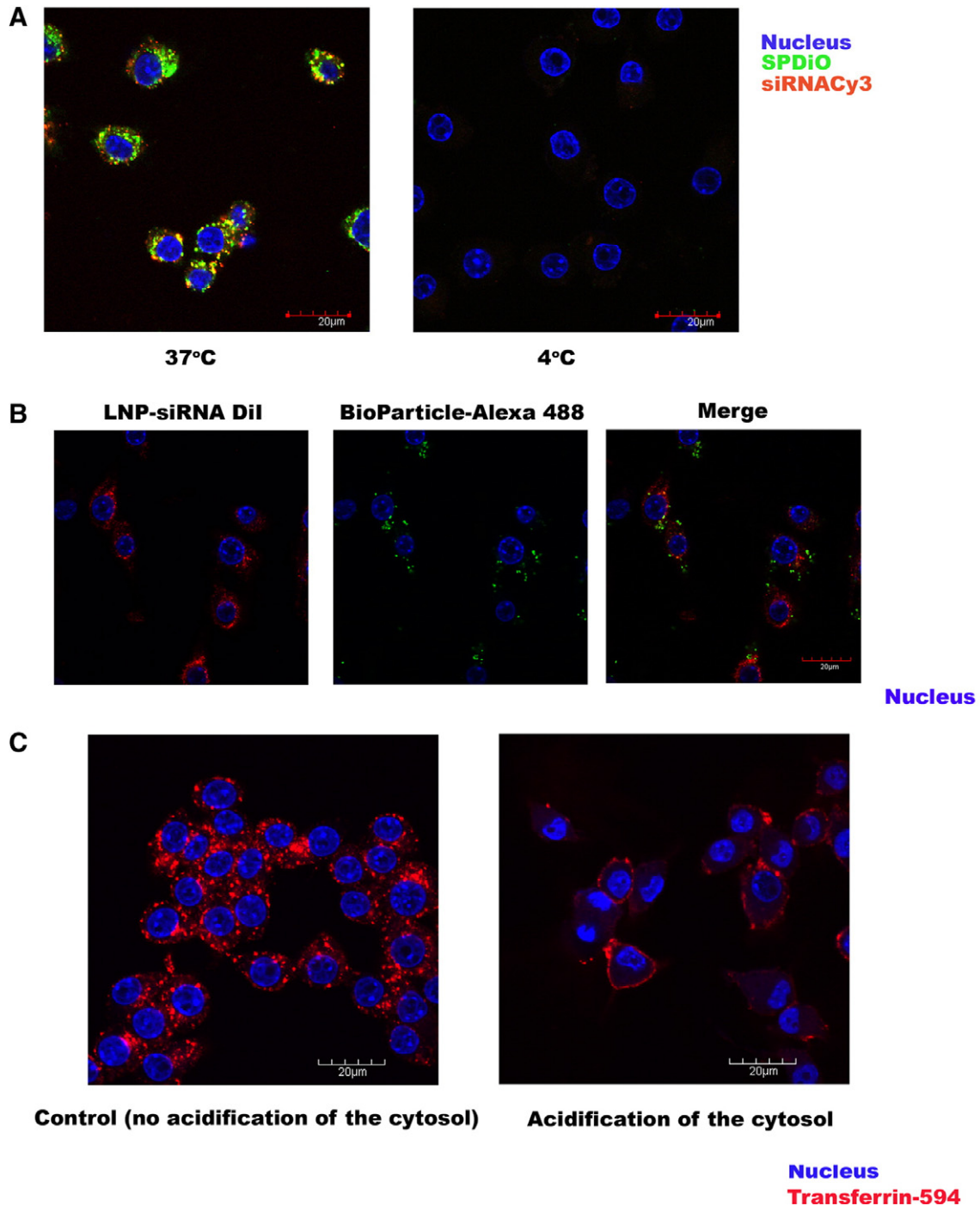
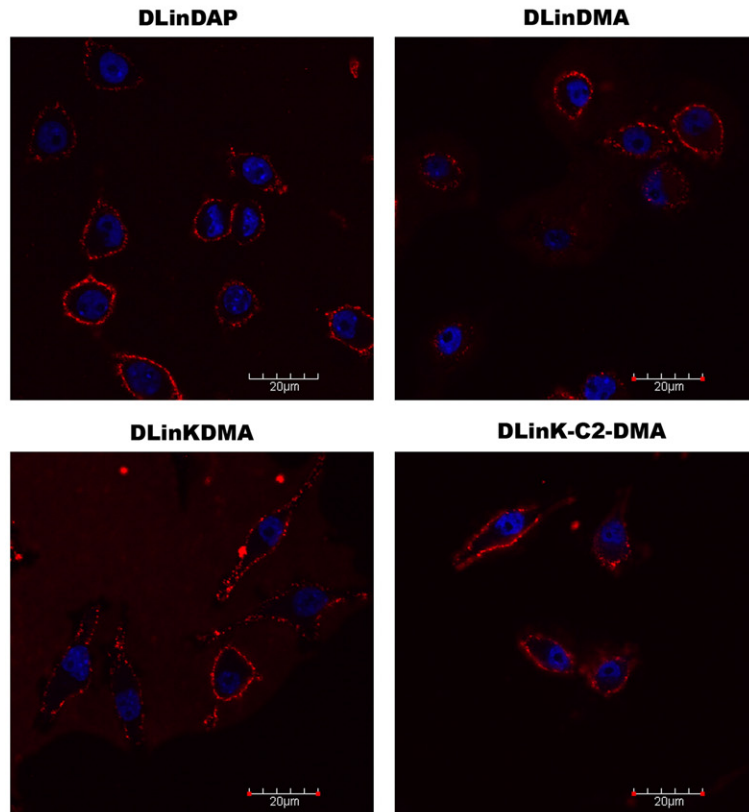


Figure 3. LNP-siRNA systems containing ionizable cationic lipids enter cells through clathrin-mediated endocytosis and macropinocytosis. **(A)** Raw 264.7 cells (2×10^5) were incubated with LNP Cy3-siRNA (1 mL; 10 μ g siRNA/mL or 700 nM) containing DLinKC2-DMA (all LNP formulations at same lipid molar ratios as in Figure 2) for 4 h at 37°C or at 4°C. A lipophilic dye, SPDio, was incorporated into the LNP to monitor uptake. The green color represents SPDio, the red color represents Cy3-siRNA, and the blue color indicates nuclear staining. **(B)** Raw 264.7 cells (2×10^5) were incubated with 1 μ g/mL Alexa 488-conjugated BioParticle, phagocytosis marker, and DLinKC2-DMA LNP-siRNA (1 mL; 10 μ g siRNA/mL or 700 nM) for 2 h at 37°C. LNPs were formulated with DiI, lipophilic dye, to monitor LNP uptake. **(C)** Raw 264.7 cells (2×10^5) were incubated with complete growth media or with complete growth media supplemented with 10 mM acetic acid at pH 5.0 for 30 min before treatment with Alexa 594-conjugated Transferrin for 6 h. **(D)** Raw 264.7 cells (2×10^5) were treated as in (C); however, cells were treated with LNP Cy3-siRNA containing DLinDAP, DLinDMA, DLinKDMA, or DLinKC2-DMA (1 mL; 10 μ g siRNA/mL or 700 nM). **(E)** Raw 264.7 cells (2×10^5) were pretreated with 200 μ M genistein, 25 μ g/mL nystatin, 10 μ g/mL chlorpromazine, or 2.5 mM amiloride for 30 min followed by treatment of cells with DLinKC2-DMA LNP-siRNA system (1 mL; 10 μ g siRNA/mL or 700 nM) for 2 h in the presence of indicated inhibitor. LNP uptake (DiI) was monitored by fluorescence microscopy. **(F)** Same as (E) with LNP-siRNA containing of DLinDAP, DLinDMA, DLinKDMA, or DLinKC2-DMA (1 mL; 10 μ g siRNA/mL or 700 nM). DiI uptake was assessed by flow cytometry.

D Acidification of the cytosol



Control (no acidification of the cytosol)

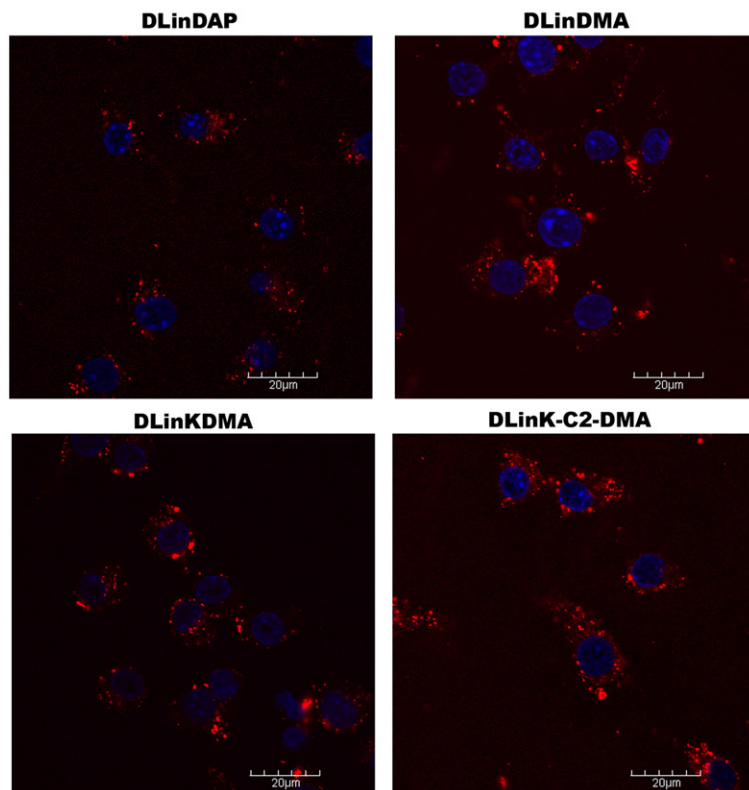


Figure 3. (continued)

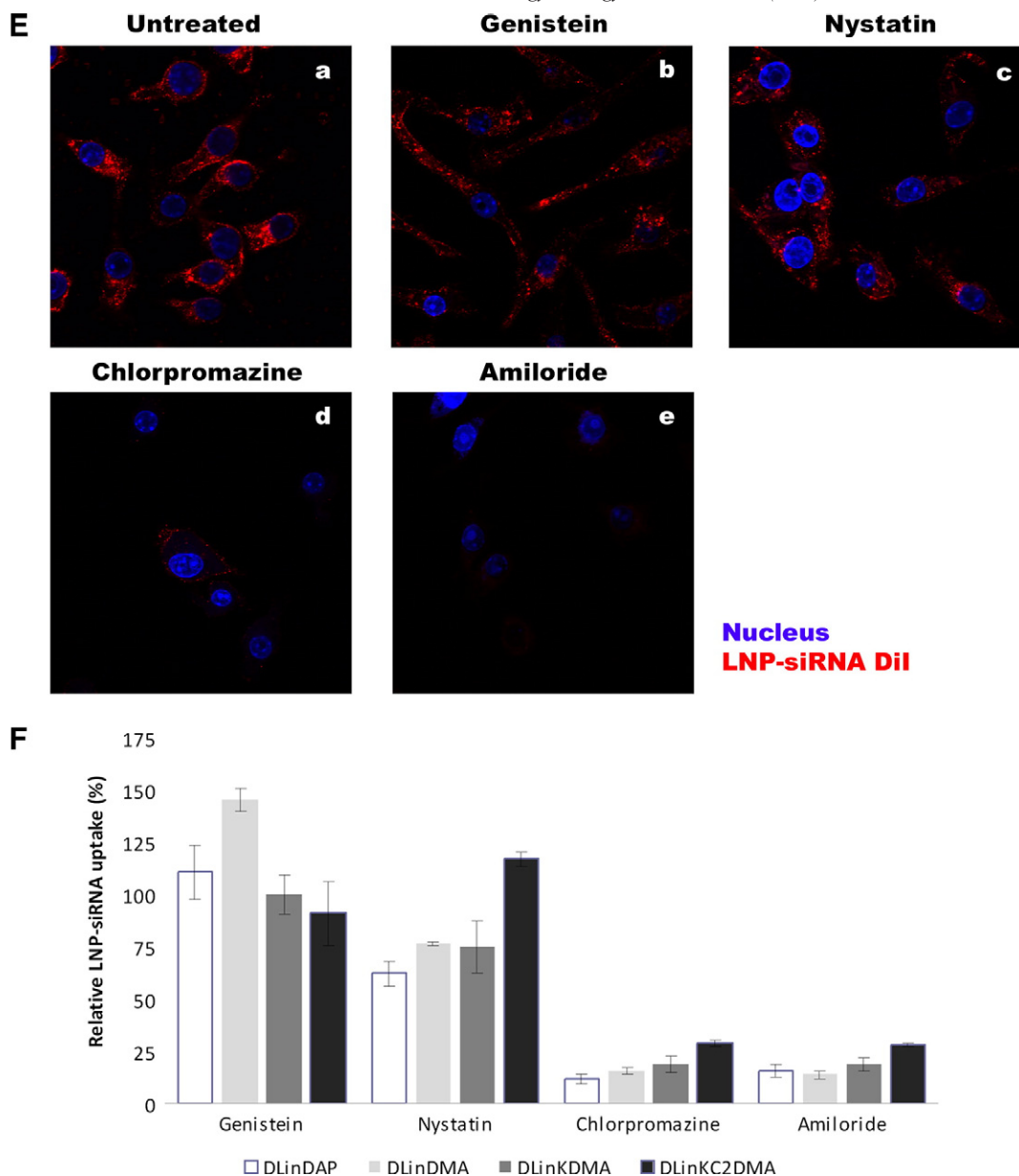


Figure 3. (continued)

Inhibitors of endocytosis

Raw 264.7 (2×10^5) cells were seeded onto a 12-well plate for 16 hours and then treated with 200 μM genistein, 25 $\mu\text{g}/\text{mL}$ nystatin, 10 $\mu\text{g}/\text{mL}$ chlorpromazine, or 2.5 mM amiloride for 30 minutes, followed by addition of 1 mL of 10 μg siRNA/mL (700 nM) LNP-siRNA for 2 hours. Cells were then harvested and washed with PBS supplemented with 2% FBS. DiI-labeled LNP-siRNA uptake in 5×10^4 Raw 264.7 cells was monitored by flow cytometry using a Becton Dickinson LSRII flow cytometer (San Jose, California). For microscopy, 2×10^5 cells were treated with inhibitors and DLinkC2-DMA LNP-siRNA systems and fixed with the protocol described above. DiI was monitored at 550 nm and images were collected sequentially using a $60\times$ oil immersion objective lens.

Fluorometric studies

Fluorometric measurements were carried out using the Luminescence Spectrometer LS50 (Perkin Elmer, Waltham, Massachusetts). The slit was maintained at 2.5 nm. Fluorometric buffer consists of 130 mM NaCl and 20 mM Hepes maintained at pH 7.47 or 4.88. Samples were stirred in buffer during measurement. Cy3 was excited at 540 nm and emission was detected at 570 nm. For Cy3-siRNA degradation assay 6 μg of Cy3-siRNA (AD1991 or AD18560) was incubated in 20 mM Tris buffer pH 6.8 and RNaseA was added at indicated time points.

In vitro stability of Cy3-siRNA

Cy3-siRNA (1 μg) was incubated in 5 $\mu\text{g}/\text{mL}$ RNaseA at 37°C for 0.5, 1, 5, 10, 20, or 30 minutes and reactions were

quenched with deionized formamide. Cy3-siRNA (0.25 µg) was resolved in a 12% denaturing urea/polyacrylamide gel and the gel was stained with $1 \times$ SybrSafe (Invitrogen) in TBE buffer for 30 minutes before visualization using a Typhoon scanner. For lipase studies, LNP Cy3-siRNA (1 µg siRNA) was incubated for 5 minutes at 37°C in the presence or absence of either 5 µg/mL RNaseA and 12 units of porcine pancreatic lipase, and fluorescence was detected with Synergy HT Multi detection plate reader (BioTek Instruments, Winooski, Vermont) or the reaction was quenched with deionized formamide and 0.25 µg of total RNA was analyzed as described above.

Statistical analyses

One-way ANOVA analysis was performed with GraphPad, followed by posttest using Tukey-Kramer Multiple Comparisons Test to evaluate significance in which probability (*P*) values must be less than 0.05.

Results

LNP-siRNA systems containing DLinKC2-DMA exhibit maximum gene silencing in a macrophage cell line

The first objective was to investigate whether LNP-siRNA systems containing ionizable cationic lipids can silence genes in a macrophage cell line and to determine which ionizable lipids were most effective. LNP systems containing DLinKC2-DMA, DLinKDMA, DLinDMA, and DLinDAP (Figure 1) and siRNA directed against GAPDH were formulated as described in *Methods*. Raw 264.7 cells were incubated with LNP GAPDH siRNA at levels corresponding to 10 µg siRNA/mL (700 nM) for up to 72 hours and analyzed for GAPDH protein levels by immunoblotting. Little or no silencing was observed at 24 hours or 48 hours (data not shown); however, pronounced GAPDH specific gene silencing was observed at 72 hours (Figure 2, A). This behavior is consistent with the long half-life of GAPDH of approximately 38 hours.²⁷ GAPDH expression was assessed from three independent experiments and a densitometric analysis of the gels was performed to provide the quantitative estimates of protein expression shown in Figure 2, B.

The results presented in Figure 2 indicate that LNP systems containing ionizable cationic lipids can silence genes in the Raw 264.7 macrophage cell line and that the relative potency of the cationic lipids varies according to DLinKC2-DMA > DLinDMA > DLinKDMA > DLinDAP. To compare the relative potency of LNP-siRNA systems consisting of different cationic lipids the LNP systems were formulated with the same size and siRNA:lipid ratio. The LNP sizes were maintained between 75–85 nm in size and the measured siRNA:lipid range was 0.085–0.091 (Table 1). Factors that can influence potency imposed by the differences of the chemical nature of the ionizable cationic lipids include the route of entry, relative levels of uptake of the LNP systems into the Raw 264.7 cells, the biodegradability of the LNP components, as well as the ability of encapsulated siRNA to escape the endosome following uptake. Experiments were conducted to investigate each of these possibilities as indicated below.

LNP-siRNA systems are accumulated into Raw 264.7 cells by clathrin mediated endocytosis and macropinocytosis

Previous work has shown that cationic lipid-based delivery systems containing plasmid^{28,29} and oligonucleotide^{30,31} accumulate in cells by endocytosis. However, recent work using LNP-siRNA delivery systems containing “lipidoid” cationic lipids has suggested entry by macropinocytosis.³² We therefore investigated the mechanism whereby the LNP used in this study are accumulated into the macrophage cell line as differences in uptake routes could influence LNP-siRNA potency. Intracellular accumulation of LNP-siRNA systems containing DLinKC2-DMA proceeded readily at 37°C as detected by the lipid label SPDiO to monitor LNP uptake and Cy3-siRNA (Figure 3, A, left); however, when the same experiment was conducted at 4°C (Figure 3, A, right) SPDiO and Cy3-siRNA were not internalized. Similar results were observed for LNP systems containing DLinKDMA, DLinDMA, and DLinDAP. This behavior is consistent with an ATP-dependent uptake process.

Raw 264.7 is a murine macrophage cell line that can internalize by phagocytosis in addition to other endocytic pathways such as clathrin-mediated endocytosis, clathrin-independent endocytosis/cholesterol-dependent endocytosis, and macropinocytosis.^{33–35} To determine whether LNP-siRNA systems are phagocytosed, colocalization studies were performed using BioParticles-Alexa 488, phagocytosis marker.^{36,37} DLinKC2-DMA LNP-siRNA systems were formulated with the lipophilic dye, DiI, to monitor LNP uptake. When Raw 264.7 cells were treated (2 hours) with the phagocytosis marker and the labeled DLinKC2-DMA LNP-siRNA system little colocalization was observed (Figure 3, B).

To determine whether LNPs entered cells through clathrin-mediated endocytosis, the cytosol of Raw 264.7 cells was first acidified by incubation with acetate, a process that interferes with budding of clathrin-coated³⁸ vesicles from the plasma membrane and trans-golgi network (TGN). In contrast to normal growth conditions where transferrin uptake, a marker for clathrin-mediated endocytosis, was readily observed (Figure 3, C, left), acidification of the cytosol blocked Alexa-594-conjugated transferrin (Tf-594) uptake resulting in the predominant cell surface distribution of Tf-594 (Figure 3, C, right). When cells were incubated with LNP Cy3-siRNA, acidification of the cytosol led to accumulation of Cy3-siRNA around the plasma membrane and little to no intracellular Cy3 fluorescence (Figure 3, D, Acidification of the cytosol) in comparison to cells treated with LNPs in complete growth media (Figure 3, D, Control—no acidification of the cytosol).

Although acidification of the cytosol directly interferes with budding of clathrin-coated pits, other endocytic pathways could be influenced by the acidic cytosolic environment. To investigate other endocytotic mechanisms, Raw 264.7 cells were pretreated with genistein (an inhibitor of caveolae-dependent and other clathrin-independent endocytosis processes), nystatin (an inhibitor of cholesterol-dependent endocytosis), chlorpromazine (an inhibitor of clathrin-mediated endocytosis), or amiloride (an inhibitor of macropinocytosis)^{39,40} as indicated

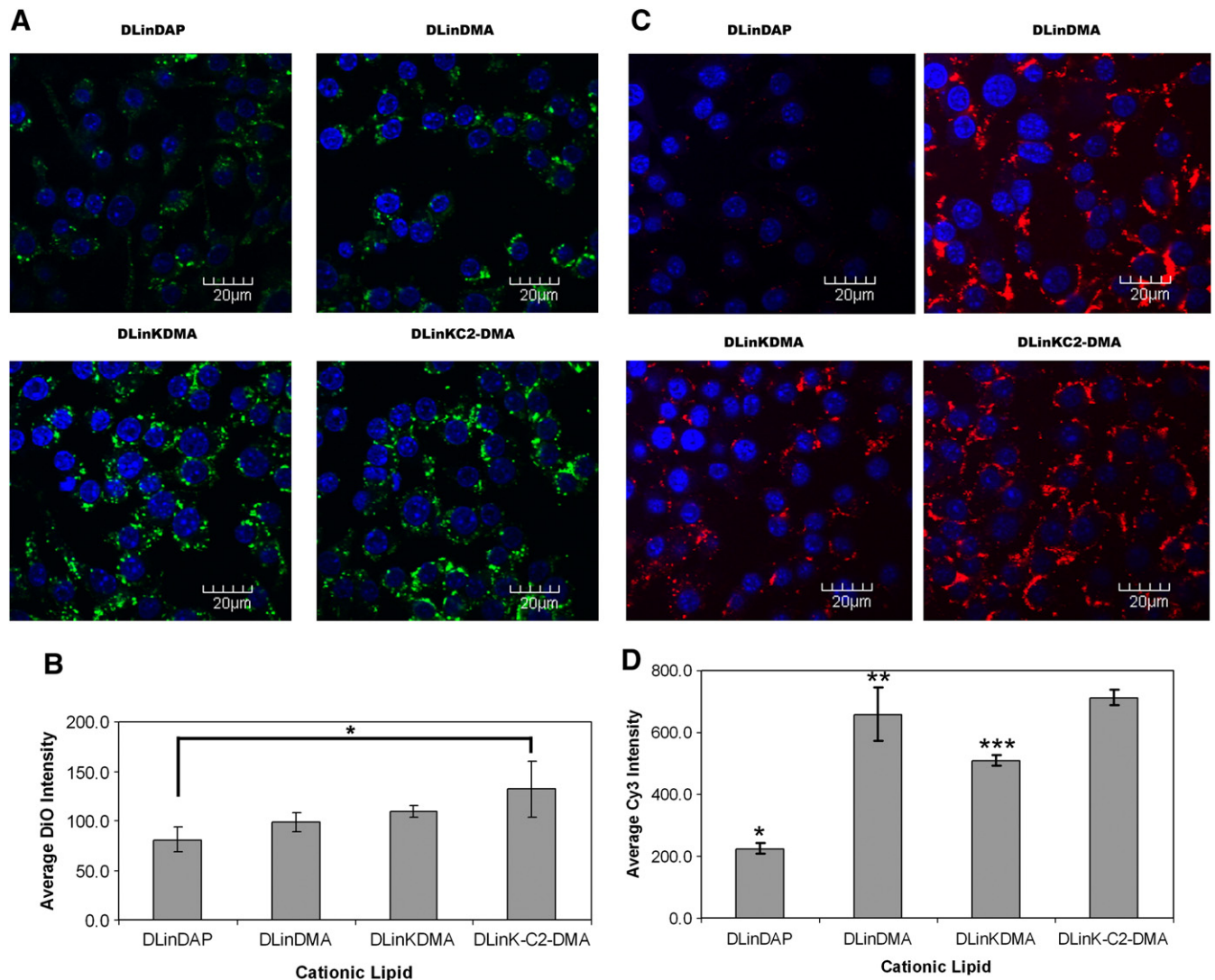


Figure 4. Influence of cationic lipid species on LNP uptake and intracellular distribution of siRNA. **(A)** Raw 264.7 cells (2×10^5) on glass cover-slips were treated for 24 h with LNP Cy3-siRNA (1 mL; 10 μ g siRNA/mL or 700 nM). LNP uptake (DiO) was visualized by confocal microscopy. **(B)** Raw 264.7 cells (10^4) were treated for 24 h with LNP Cy3-siRNA (100 μ L; 10 μ g siRNA/mL or 700 nM) and assessed for SPDio fluorescence using the Cellomics ArrayScan VTI. ANOVA analysis/Tukey-Kramer multiple comparisons test was performed. Only DLinDAP versus DLinKC2-DMA showed significance $*P < 0.05$. **(C)** Raw 264.7 cells (2×10^5) were treated for 24 h with LNP Cy3-siRNA (1 mL; 10 μ g siRNA/mL or 700 nM). Cy3-siRNA accumulation was visualized by confocal microscopy. **(D)** Raw 264.7 cells (10^4) were treated for 24 h with LNP Cy3-siRNA (100 μ L; 10 μ g siRNA/mL or 700 nM) and assessed for Cy3 fluorescence using the Cellomics ArrayScan VTI. ANOVA analysis/Tukey-Kramer Multiple comparisons test was performed. *DLinDAP versus DLinDMA, DLinKDMA, or DLinKC2-DMA $P < 0.001$, **DLinDMA versus DLinKDMA $P < 0.05$, DLinDMA versus DLinKC2-DMA NS, ***DLinKDMA versus DLinKC2-DMA $P < 0.01$. **(E)** The distribution of Cy3-siRNA was further analyzed by confocal microscopy. Micrographs *a-d* show Cy3-siRNA distribution at 60 \times oil immersion with 2 \times magnification. Micrographs *e-h* show 180% magnification of selected cells in *a-d*. Scale bar: 20 μ m.

under *Methods*. Genistein and nystatin did not inhibit the internalization of DLinKC2-DMA LNP-siRNA systems (Figure 3, E, b,c) as compared with control (Figure 3, E, a). Uptake was reduced when treated with chlorpromazine (Figure 3, E, d) and amiloride (Figure 3, E, e). To determine whether the species of cationic lipid influenced the internalization, the uptake of DLinDAP, DLinDMA, and DLinKDMA LNP-siRNA systems were monitored by flow cytometry in the presence of endocytic inhibitors. Again, internalization was predominantly driven by clathrin-mediated endocytosis and macropinocytosis (Figure 3, F).

Delivery of intact siRNA to the cell cytoplasm is significantly improved for LNP-siRNA systems containing DLinKC2-DMA

The next factor investigated concerned LNP uptake and cytoplasmic delivery of siRNA. The intracellular accumulation of SPDio was similar for cells treated with DLinDAP, DLinDMA, and DLinKDMA LNP systems and slightly higher for cells treated with LNP containing DLinKC2-DMA (Figure 4, A). Similar results were obtained by measuring the average fluorescent intensity per cell using the Cellomics ArrayScan (Figure 4, B).

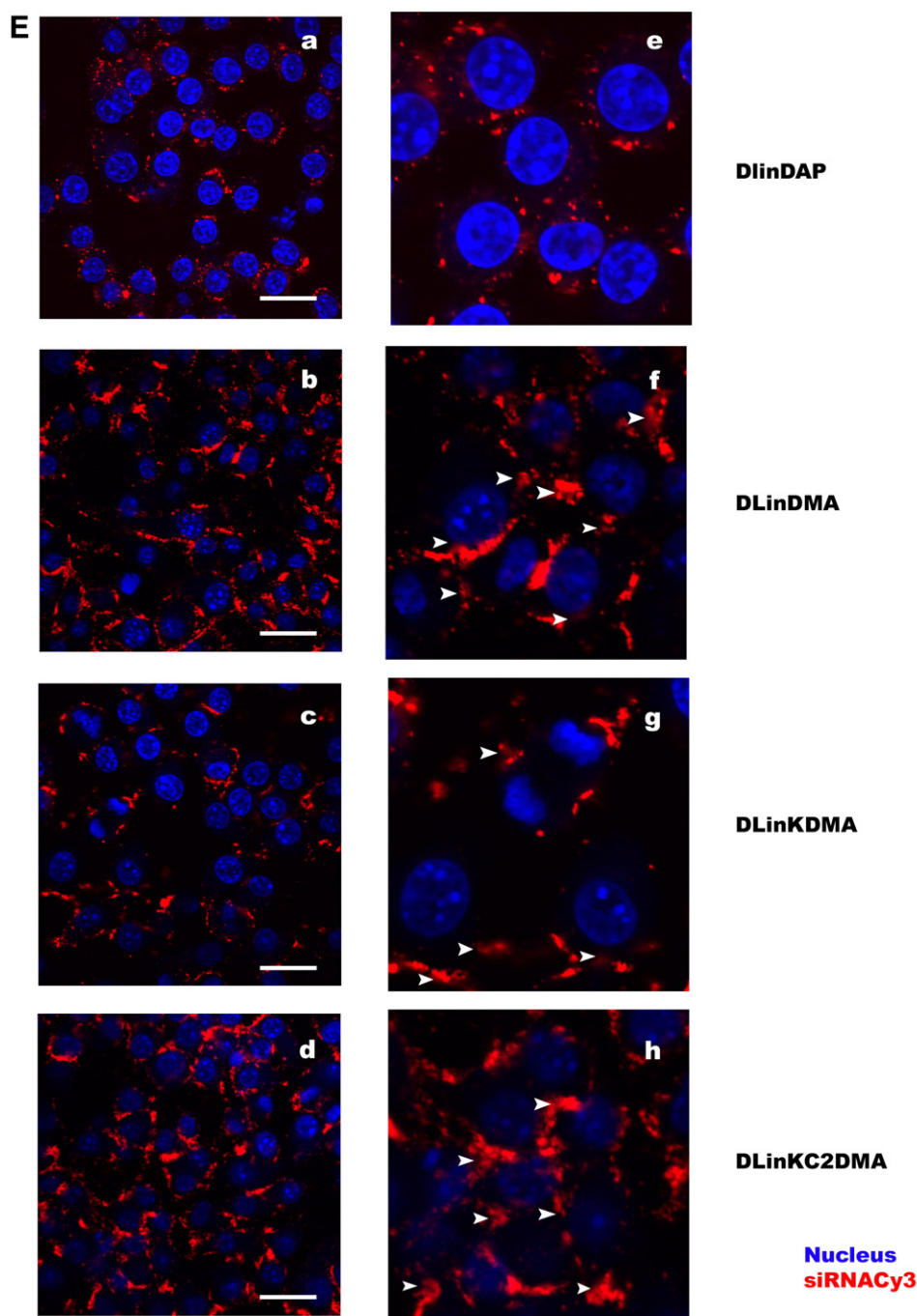
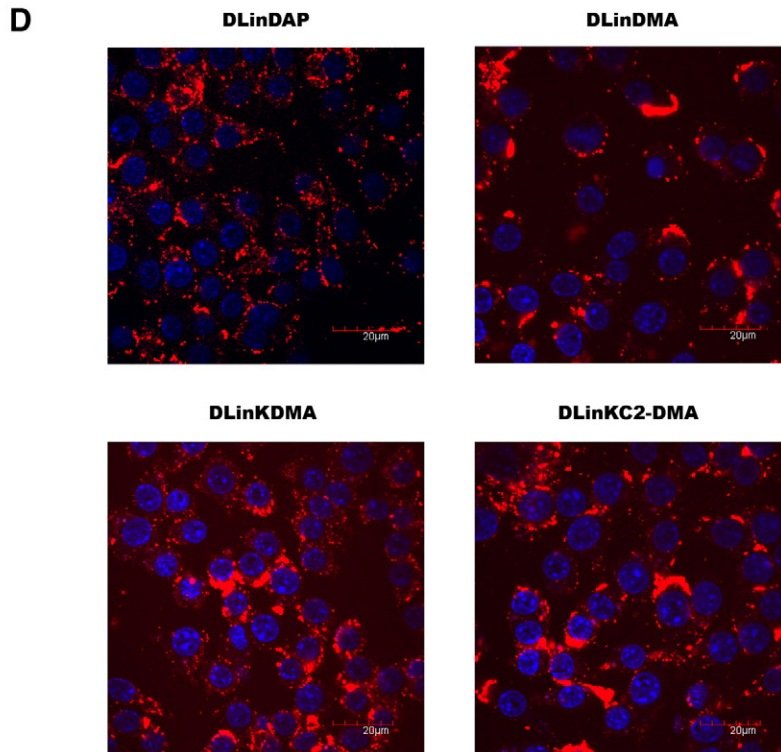
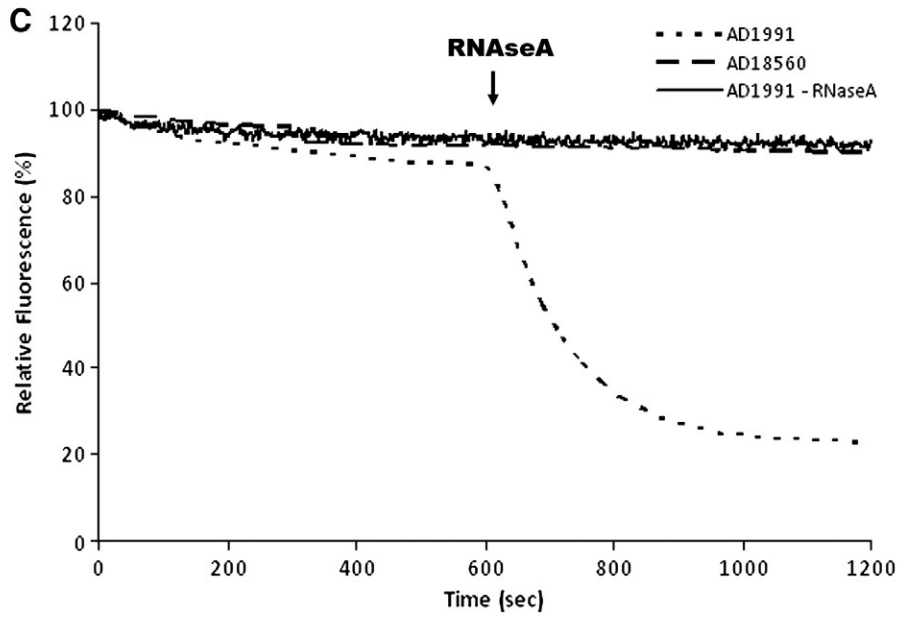
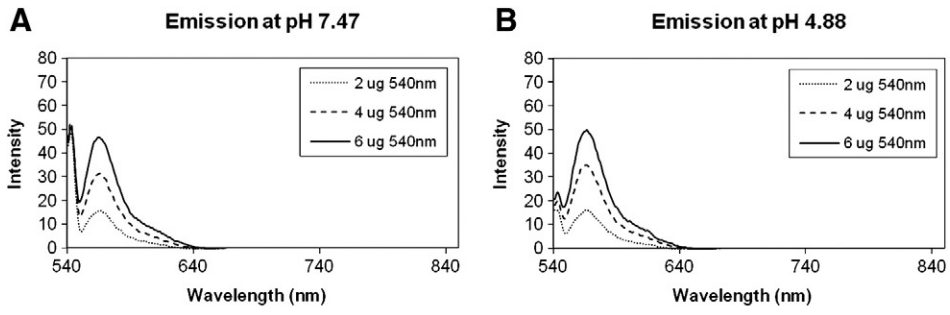


Figure 4. (continued)

The next set of experiments was designed to monitor uptake of LNP-siRNA using fluorescently labeled siRNA (Cy3-siRNA) as opposed to fluorescently labeled lipid. In contrast to the results obtained using SPDiO, the accumulation of Cy3-siRNA was significantly dependent on the species of ionizable cationic lipid present in the LNP. Accumulation of Cy3-siRNA was readily detected for DLinDMA and DLinKC2-DMA LNP systems, was somewhat reduced for LNP containing DLinKDMA, and was much reduced for LNP containing

DLinDAP (Figure 4, C and D). In addition, inspection of the intracellular distribution of accumulated Cy3-siRNA revealed a dependence on the cationic lipid used (Figure 4, E, e). In particular, Cy3-siRNA presented in DLinDAP LNPs exhibited primarily punctate intracellular features (Figure 4, E, e), whereas Cy3-siRNA delivered in DLinDMA, DLinKDMA, and DLinKC2-DMA LNP systems also showed a diffuse background Cy3-siRNA signal consistent with an enhanced cytosolic distribution (Figure 4, E, f,g,h, arrows).



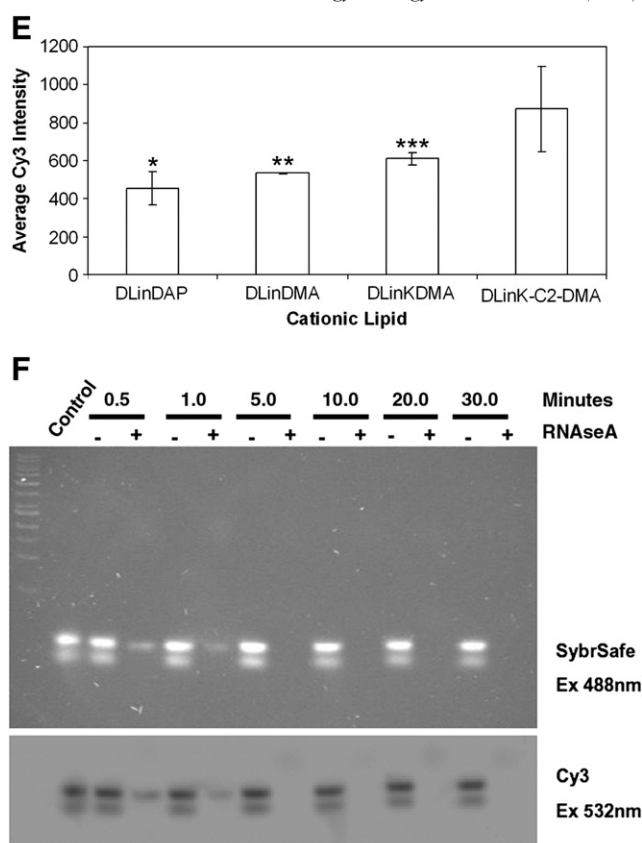


Figure 5. The fluorescence intensity arising from Cy3-siRNA AD1991 is dependent on the integrity of the siRNA oligonucleotide. (A) Cy3-siRNA intensity at pH 7.47. (B) Cy3-siRNA intensity at pH 4.88. (C) The fluorescence of Cy3-siRNA (6 μg) monitored for 20 min in the presence of RNaseA (AD1991 dotted line; 18560 dashed line) or in the absence of RNaseA (AD1991 - RNaseA solid line). (D) Raw 264.7 cells (2×10^5) were treated with LNP AD18560 Cy3-siRNA for 24 h (1 mL; 10 μg siRNA/mL or 700 nM). Cy3-siRNA accumulation was visualized by confocal microscopy. (E) Raw 264.7 cells (10^4) were treated with LNP AD18560 Cy3-siRNA for 24 h (100 μL ; 10 μg siRNA/mL or 700 nM). Cy3 fluorescence was assessed with the Cellomics ArrayScan VTI. ANOVA analysis/Tukey-Kramer Multiple comparisons test was performed. *DLinDAP versus DLinDMA and DLinkDMA NS (not significant), DLinDAP versus DLinkC2-DMA $P < 0.01$, **DLinDMA versus DLinkDMA NS, DLinDMA versus DLinkC2-DMA $P < 0.05$, ***DLinKDMA versus DLinkC2-DMA NS. (F), Cy3-siRNA (AD1991) \pm RNaseA was incubated at 37°C and analyzed with the Typhoon scanner at 488 nm (Sybr Safe staining) and 564 nm (Cy3).

Fluorescent intensity measurements indicate Cy3-labeled siRNA is more readily degraded when delivered by DLinDAP systems

In the course of the experiments detailed in the previous section, it was consistently observed that the intracellular fluorescent intensity for Cy3-siRNA delivered in LNP containing DLinDAP was significantly lower than observed for LNP containing DLinDMA, DLinkDMA, or DLinkC2-DMA (Figure 4, D). This contrasted with uptake monitored by SPDiO fluorescence, which was relatively independent of cationic lipid composition (Figure 4, B). The fluorescent intensity of the Cy3-labeled siRNA emission spectra was also pH independent over the range pH 4.9 and pH 7.5 (Figure 5, A and B), indicating that changes in endosomal pH were not causing the change in fluorescence.

As discussed in Sanborn et al⁴¹ the fluorescence lifetime of Cy3 when conjugated to an oligonucleotide (2 ns) is 10 times longer than free Cy3 (0.18 ns).⁴¹ The siRNA used in Figure 4 consists of siRNA-Cy3 AD1991. The Cy3 label in the AD1991 sequence is conjugated to an unmodified uracil residue therefore susceptible to nuclease digestion (Table 2). As shown in

Table 2
Cy3-siRNA sequences

Designation	Strand	Sequence
AD1991	Sense	5' - cuuAcGcu GAGu Acuuc GAdTsdT - 3'
	Antisense	5' - Cy3-UCGAAGu ACu cAGCGuAAGdTsdT - 3'
AD18560	Sense	5' - GGAAUC uu Au Auuu GAUCcAsA - 3'
	Antisense	5' - Cy3- uu GGAUc AAA Au AAG AuUC cs sU - 3'

Non-capitalized bold residues (u, c, s) indicate 2'O-methyl modification.

Figure 5, C, when the Cy3-siRNA AD1991 was incubated with RNaseA, the fluorescence signal from AD1991 was reduced over time, whereas no fluorescence decrease was observed in the absence of nuclease. As a control, a second Cy3-siRNA was generated (sequence AD18560, Table 2) where the Cy3-label is conjugated to a 2'O-methylated uracil residue, which confers nuclease resistance. In the presence of RNaseA AD18560 showed no loss of Cy3 fluorescence (Figure 5, C). These observations indicate that loss of Cy3 fluorescence for the

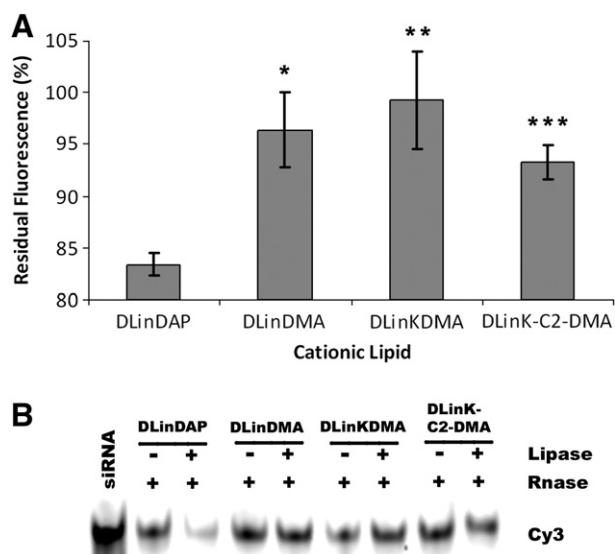


Figure 6. Incubation of LNP-siRNA systems containing DLinDAP with lipase renders the encapsulated siRNA susceptible to nuclease attack. **(A)** LNP encapsulated Cy3-siRNA (1 μ g siRNA) was incubated at 37°C in the presence or absence of RNaseA and/or pancreatic lipase for 5 min and Cy3 fluorescence was measured. Relative Cy3 fluorescence was measured from three independent experiments \pm standard deviations. ANOVA analysis/Tukey-Kramer Multiple comparisons test was performed. DLinDAP versus DLinDMA $*P < 0.01$, DLinDAP versus DLinKDMA $**P < 0.001$, DLinDAP versus DLinKC2-DMA $***P < 0.05$. **(B)** Encapsulated Cy3-siRNA (1 μ g) was treated with RNaseA or RNaseA + lipase for 5 min and analyzed at 564 nm with the Typhoon scanner.

AD1991 sequence is associated with nuclease-induced breakdown of the oligonucleotide.

If the loss in fluorescence of Cy3-siRNA (sequence AD1991) is due to degradation following uptake, it would be expected that there would be no loss of fluorescence if the non-degradable sequence (sequence AD18560) was delivered in the LNP-siRNA systems containing DLinDAP. To demonstrate that this is the case Cy3-siRNA AD18560 was encapsulated in DLinDAP LNP and incubated (24 hours) with Raw 264.7 cells. As shown in Figure 5, D and E, Cy3-siRNA accumulated at similar levels for all LNP systems, with the exception that LNP containing DLinKC2-DMA showed higher accumulation, in agreement with uptake levels monitored by the fluorescent lipid SPDiO (Figure 4, B).

To definitively demonstrate that a reduction of the Cy3 fluorescent intensity for sequence AD1991 is a direct consequence of siRNA breakdown, it was observed that within 5 minutes of incubation in the presence of RNaseA the AD1991 band was completely eliminated (Figure 5, F, top), correlating with the loss of Cy3 signal (Figure 5, F, bottom).

Degradation of Cy3-labeled siRNA by RNaseA in LNP systems containing DLinDAP is enabled by exposure to lipase

The next question concerns why Cy3-siRNA (AD1991) in the LNP-siRNA system containing DLinDAP was susceptible to degradation following uptake into the macrophage cell line, whereas Cy3-siRNA (AD1991) encapsulated in LNP systems

Table 3

Gene silencing activities of LNP-siRNA systems normalized to uptake levels

Residual GAPDH		Cationic lipid
Normalized to uptake (DiO)	Normalized to Cy3 (AD18560)	
1	1	DLinDAP
0.373	0.389	DLinDMA
0.539	0.544	DLinKDMA
0.189	0.161	DLinKC2-DMA

containing DLinDMA, DLinKDMA, or DLinKC2-DMA was not. A distinguishing feature of DLinDAP is the presence of ester linkages between the head group and the acyl chains, which could be susceptible to degradation by endogenous esterases and lipases present in endosomes.^{42–44}

As shown in Figure 6, A, significant RNaseA degradation of Cy3-siRNA (AD1991) encapsulated in DLinDAP LNPs was observed when lipase was present, whereas Cy3-siRNA (AD1991) in LNP systems composed of DLinDMA, DLinKDMA, and DLinKC2-DMA was protected. Released Cy3 following degradation can still contribute to overall fluorescence, leading to high background levels. The effects of RNaseA on encapsulated Cy3-siRNA (AD1991) were therefore visualized by gel electrophoresis as shown in Figure 6, B. In the absence of lipase, all the LNP systems protected encapsulated Cy3-siRNA against RNaseA digestion. However, following incubation of LNP with pancreatic lipase and RNaseA, only 25% of intact Cy3-siRNA was observed for LNP containing DLinDAP after 5 minutes (Figure 6, B). This contrasts with the behavior of LNP containing DLinDMA, DLinKDMA, or DLinKC2-DMA, which protected their siRNA payloads under similar conditions (Figure 6, B).

Discussion

This work demonstrates that LNP-siRNA systems containing ionizable cationic lipids can silence target genes in the macrophage cell line Raw 264.7 and that differences in transfection potency can be attributed to differing levels of uptake, differing stabilities of the cationic lipid following uptake as well as differing abilities to escape the endocytotic pathway. There are three areas that deserve further discussion including the reasons for the different gene silencing potencies of LNP containing different species of cationic lipid, the use of the assay described in this study to detect siRNA breakdown following uptake into cells and the implications of this work for the development of improved LNP-siRNA delivery systems.

It is clear from the results presented in this study that the relative impotency of the LNP systems containing DLinDAP can be attributed, at least in part, to the degradation of DLinDAP by endogenous lipases. This will reduce the availability of DLinDAP for promoting endosomal escape as well as render encapsulated siRNA sensitive to degradation by nucleases. It is most probable that LNP systems are degraded subsequent to cellular uptake because nucleases and lipases (esterases) are absent from growth media but are present in endocytic and lysosomal compartments.^{43,45} The surprising feature is how rapidly the DLinDAP must be degraded following uptake, before

sufficient acidification takes place for the cationic lipid to effect endosomal escape. It would be expected that accumulated LNP will be exposed to pH environments below pH 5.5 within an hour or much less.⁴⁶ In such an environment the DLinDAP, which exhibits a pKa of 6.2,¹² would be fully protonated and show comparable membrane destabilization activity as DLinKC2-DMA in the presence of endogenous acidic lipids. As noted in Figure 6, A and B, LNP-siRNA systems containing DLinDMA, DLinKDMA, and DLinKC2-DMA are not susceptible to lipase attack, consistent with increased stability of encapsulated siRNA following uptake into the Raw 264.7 cells and increased gene silencing potency.

The differences in gene silencing potencies observed between DLinDMA, DLinKDMA, and DLinKC2-DMA clearly arise, at least in part, from the enhanced accumulation of LNP-siRNA systems containing DLinDMA and DLinKC2-DMA as compared with LNP containing DLinKDMA. As shown in Figure 4, D, DLinKDMA LNPs exhibited 25–30% lower uptake levels, as indicated by Cy3-siRNA, in comparison to DLinDMA and DLinKC2-DMA LNPs. The reason why DLinKC2-DMA exhibits enhanced gene silencing properties as compared with DLinDMA is not obvious from inspection of the distribution of Cy3-siRNA delivered by LNP containing DLinKC2-DMA as compared with LNP containing DLinDMA (Figure 4, E, f and h). There is no clear indication of enhanced intracellular delivery (as evidenced by a diffuse fluorescent background) by DLinKC2-DMA as compared with DLinDMA. However, if the gene silencing potencies are normalized to uptake of either of the non-degradable fluorescent markers (DiO and Cy3-siRNA AD18560) as shown in Table 3, it is clear that DLinKC2-DMA has enhanced gene silencing potency as compared with DLinDMA that cannot be accounted for solely by uptake levels. It is probable that this arises from enhanced endosomolytic properties as indicated by the enhanced ability of DLinKC2-DMA to destabilize bilayer structure in mixtures with anionic lipids as compared with DLinDMA in vitro.¹² As noted elsewhere,⁴⁷ cationic lipids combine with endogenous anionic lipids to produce ion pairs that are very potent bilayer destabilizing agents.

The assay described in this study to follow degradation of siRNA following uptake into cells by following the loss in fluorescence of Cy3-labeled siRNA clearly has use for characterizing the fate of siRNA delivered by nanoparticulate carriers into cells as a function of carrier composition, particularly the susceptibility of components, such as cationic lipids, to degradation. In general, it should be noted that the results presented in this study suggest considerable use for in vitro assays of LNP-siRNA gene silencing potency as being predictive of in vivo behavior. The relative potency of LNP-siRNA systems in the macrophage cell line used in this study followed the series DLinKC2-DMA > DLinDMA > DLinKDMA >> DLinDAP, similar to the behavior observed in vivo where DLinKC2-DMA > DLinKDMA > DLinDMA >> DLinDAP for LNP-siRNA-induced silencing in the liver (hepatocytes) following iv administration. The reason why DLinDMA is somewhat more potent than DLinKDMA in vitro but less potent in vivo could arise because of the higher pKa of DLinDMA as compared with DLinKDMA (6.8 versus 5.9¹²). The higher pKa will result

in a higher surface charge for LNP containing DLinDMA, which would be expected to encourage association with the negatively charged membrane of the macrophage cell line in vitro and thus enhance uptake, but would also engender increased association of serum proteins in vivo, leading to faster clearance by the RES and reducing delivery to target hepatocyte cells.

The implications of the work described in this study for the design of LNP-siRNA systems that give improved gene silencing properties in vivo are twofold. First, the gene silencing properties of LNP-siRNA systems may be usefully screened using in vitro systems where gene silencing properties are normalized to uptake levels to reveal endosomal escape/cytoplasmic delivery features. Second, macrophage cell lines such as used in this study may be usefully used to screen for LNP-siRNA systems with improved potency for silencing genes in macrophages and possibly other APCs following iv injection. Studies have shown that silencing can be achieved in macrophages and dendritic cells in vivo following iv administration of LNP-siRNA systems containing DLinKC2-DMA.¹⁴ However, the dose levels required (5 mg siRNA/kg body weight) are much higher than those required to silence genes in hepatocytes following iv administration, where only 0.01 mg siRNA/kg body weight is required.¹² The high potency of LNP-siRNA systems for hepatocyte gene silencing has been attributed to association with apolipoprotein E, which leads to uptake through the scavenging receptor.⁴⁸ This suggests that screening for targeting ligands that encourage uptake of LNP-siRNA systems into macrophages and other APCs in vitro should have direct application to the in vivo situation.

References

1. Lares MR, Rossi JJ, Ouellet DL. RNAi and small interfering RNAs in human disease therapeutic applications. *Trends Biotechnol* 2010;**28**: 570–9.
2. Zhang S, Zhao B, Jiang H, Wang B, Ma B. Cationic lipids and polymers mediated vectors for delivery of siRNA. *J Control Release* 2007;**123**:1–10.
3. Allen TM, Cullis PR. Drug delivery systems: entering the mainstream. *Science* 2004;**303**:1818–22.
4. Raney SG, Wilson KD, Sekirov L, Chikh G, de Jong SD, Cullis PR, et al. The effect of circulation lifetime and drug-to-lipid ratio of intravenously administered lipid nanoparticles on the biodistribution and immunostimulatory activity of encapsulated CpG-ODN. *J Drug Targeting* 2008;**16**:564–77.
5. Wilson KD, de Jong SD, Kazem M, Lall R, Hope MJ, Cullis PR, et al. The combination of stabilized plasmid lipid particles and lipid nanoparticle encapsulated CpG containing oligodeoxynucleotides as a systemic genetic vaccine. *J Gene Med* 2009;**11**:14–25.
6. Wheeler JJ, Palmer L, Ossanlou M, MacLachlan I, Graham RW, Zhang YP, et al. Stabilized plasmid-lipid particles: construction and characterization. *Gene Ther* 1999;**6**:271–81.
7. Ambegia E, Ansell S, Cullis P, Heyes J, Palmer L, MacLachlan I. Stabilized plasmid-lipid particles containing PEG-dialcylglycerols exhibit extended circulation lifetimes and tumor selective gene expression. *Biochim Biophys Acta* 2005;**1669**:155–63.
8. Maurer N, Wong KF, Stark H, Louie L, McIntosh D, Wong T, et al. Spontaneous entrapment of polynucleotides upon electrostatic interaction with ethanol-destabilized cationic liposomes. *Biophys J* 2001;**80**: 2310–26.

9. Semple SC, Klimuk SK, Harasym TO, Dos Santos N, Ansell SM, Wong KF, et al. Efficient encapsulation of antisense oligonucleotides in lipid vesicles using ionizable aminolipids: formation of novel small multilamellar vesicle structures. *Biochim Biophys Acta* 2001;**1510**: 152–66.
10. Akinc A, Zumbuehl A, Goldberg M, Leshchiner ES, Busini V, Hossain N, et al. A combinatorial library of lipid-like materials for delivery of RNAi therapeutics. *Nat Biotechnol* 2008;**26**:561–9.
11. Zimmermann TS, Lee AC, Akinc A, Bramlage B, Bumcrot D, Fedoruk MN, et al. RNAi-mediated gene silencing in non-human primates. *Nature* 2006;**441**:111–4.
12. Semple SC, Akinc A, Chen J, Sandhu AP, Mui BL, Cho CK, et al. Rational design of cationic lipids for siRNA delivery. *Nat Biotechnol* 2010;**28**:172–6.
13. Lee JB, Zhang K, Tam YY, Tam YK, Belliveau NM, Sung VY, et al. Lipid nanoparticle siRNA systems for silencing the androgen receptor in human prostate cancer in vivo. *Int J Cancer* 2012;**131**:e781–90.
14. Basha G, Novobrantseva TI, Rosin N, Tam YY, Hafez IM, Wong MK, et al. Influence of cationic lipid composition on gene silencing properties of lipid nanoparticle formulations of siRNA in antigen-presenting cells. *Mol Ther* 2011;**19**:2186–200.
15. Chonn A, Semple SC, Cullis PR. Association of blood proteins with large unilamellar liposomes in vivo: relation to circulation lifetimes. *J Biol Chem* 1992;**267**:18759–65.
16. Chonn A, Semple SC, Cullis PR. Beta 2 glycoprotein I is a major protein associated with very rapidly cleared liposomes in vivo, suggesting a significant role in the immune clearance of “non-self” particles. *J Biol Chem* 1995;**270**:25845–9.
17. Peters MJ, van Sijl AM, Voskuyl AE, Sattar N, Smulders YM, Nurmohamed MT. The effects of tumor necrosis factor inhibitors on cardiovascular risk in rheumatoid arthritis. *Curr Pharm Des* 2012;**18**: 1502–11.
18. Peters MJ, Welsh P, McInnes IB, Wolbink G, Dijkmans BA, Sattar N, et al. Tumour necrosis factor alpha blockade reduces circulating N-terminal pro-brain natriuretic peptide levels in patients with active rheumatoid arthritis: results from a prospective cohort study. *Ann Rheum Dis* 2010;**69**:1281–5.
19. Kim SS, Ye C, Kumar P, Chiu I, Subramanya S, Wu H, et al. Targeted delivery of siRNA to macrophages for anti-inflammatory treatment. *Mol Ther* 2010;**18**:993–1001.
20. Zheng X, Suzuki M, Zhang X, Ichim TE, Zhu F, Ling H, et al. RNAi-mediated CD40-CD154 interruption promotes tolerance in autoimmune arthritis. *Arthritis Res Ther* 2010;**12**:R13.
21. Odobasic D, Leech MT, Xue JR, Holdsworth SR. Distinct in vivo roles of CD80 and CD86 in the effector T-cell responses inducing antigen-induced arthritis. *Immunology* 2008;**124**:503–13.
22. Wang CY, Mazer SP, Minamoto K, Takuma S, Homma S, Yellin M, et al. Suppression of murine cardiac allograft arteriopathy by long-term blockade of CD40-CD154 interactions. *Circulation* 2002;**105**:1609–14.
23. Pilat N, Sayegh MH, Wekerle T. Costimulatory pathways in transplantation. *Semin Immunol* 2011;**23**:293–303.
24. Gizinski AM, Fox DA, Sarkar S. Pharmacotherapy: concepts of pathogenesis and emerging treatments. Co-stimulation and T cells as therapeutic targets. *Best Pract Res Clin Rheumatol* 2010;**24**:463–77.
25. Felix NJ, Suri A, Salter-Cid L, Nadler SG, Gujrathi S, Corbo M, et al. Targeting lymphocyte co-stimulation: from bench to bedside. *Autoimmunity* 2010;**43**:514–25 [Review].
26. Reynolds A, Leake D, Boese Q, Scaringe S, Marshall WS, Khvorova A. Rational siRNA design for RNA interference. *Nat Biotechnol* 2004;**22**: 326–30.
27. Franch HA, Sooparb S, Du J, Brown NS. A mechanism regulating proteolysis of specific proteins during renal tubular cell growth. *J Biol Chem* 2001;**276**:19126–31.
28. Almofti MR, Harashima H, Shinohara Y, Almofti A, Baba Y, Kiwada H. Cationic liposome-mediated gene delivery: biophysical study and mechanism of internalization. *Arch Biochem Biophys* 2003;**410**:246–53.
29. Briane D, Lesage D, Cao A, Coudert R, Lievre N, Salzman JL, et al. Cellular pathway of plasmids vectorized by cholesterol-based cationic liposomes. *J Histochem Cytochem* 2002;**50**:983–91.
30. Yotsumoto S, Saegusa K, Aramaki Y. Endosomal translocation of CpG-oligodeoxynucleotides inhibits DNA-PKcs-dependent IL-10 production in macrophages. *J Immunol* 2008;**180**:809–16.
31. Zelphati O, Szoka Jr FC. Intracellular distribution and mechanism of delivery of oligonucleotides mediated by cationic lipids. *Pharm Res* 1996;**13**:1367–72.
32. Love KT, Mahon KP, Levins CG, Whitehead KA, Querbes W, Dorkin JR, et al. Lipid-like materials for low-dose, in vivo gene silencing. *Proc Natl Acad Sci U S A* 2010;**107**:1864–9.
33. Franca A, Aggarwal P, Barsov EV, Kozlov SV, Dobrovolskaia MA, Gonzalez-Fernandez A. Macrophage scavenger receptor A mediates the uptake of gold colloids by macrophages in vitro. *Nanomedicine* 2011;**6**: 1175–88.
34. Gu J, Xu H, Han Y, Dai W, Hao W, Wang C, et al. The internalization pathway, metabolic fate and biological effect of superparamagnetic iron oxide nanoparticles in the macrophage-like RAW264.7 cell. *Sci China Life Sci* 2011;**54**:793–805.
35. Yao W, Li K, Liao K. Macropinocytosis contributes to the macrophage foam cell formation in RAW264.7 cells. *Acta Biochim Biophys Sinica* 2009;**41**:773–80.
36. Klein RD, Su GL, Schmidt C, Aminlari A, Steintraesser L, Alarcon WH, et al. Lipopolysaccharide-binding protein accelerates and augments *Escherichia coli* phagocytosis by alveolar macrophages. *J Surg Res* 2000;**94**:159–66.
37. Shibata T, Nagata K, Kobayashi Y. The mechanism underlying the appearance of late apoptotic neutrophils and subsequent TNF-alpha production at a late stage during *Staphylococcus aureus* bioparticle-induced peritoneal inflammation in inducible NO synthase-deficient mice. *Biochim Biophys Acta* 2010;**1802**:1105–11.
38. Hansen SH, Sandvig K, van Deurs B. Clathrin and HA2 adaptors: effects of potassium depletion, hypertonic medium, and cytosol acidification. *J Cell Biol* 1993;**121**:61–72.
39. Shamsul HM, Hasebe A, Iyori M, Ohtani M, Kiura K, Zhang D, et al. The Toll-like receptor 2 (TLR2) ligand FSL-1 is internalized via the clathrin-dependent endocytic pathway triggered by CD14 and CD36 but not by TLR2. *Immunology* 2010;**130**:262–72.
40. Vercauteren D, Vandenbroucke RE, Jones AT, Rejman J, Demeester J, De Smedt SC, et al. The use of inhibitors to study endocytic pathways of gene carriers: optimization and pitfalls. *Mol Ther* 2010;**18**:561–9.
41. Sanborn ME, Connolly BK, Gurunathan K, Levitus M. Fluorescence properties and photophysics of the sulfoindocyanine Cy3 linked covalently to DNA. *J Physical Chem* 2007;**111**:11064–74.
42. Heeren J, Grewal T, Jackle S, Beisiegel U. Recycling of apolipoprotein E and lipoprotein lipase through endosomal compartments in vivo. *J Biol Chem* 2001;**276**:42333–8.
43. Hornick CA, Thouron C, DeLamatre JG, Huang J. Triacylglycerol hydrolysis in isolated hepatic endosomes. *J Biol Chem* 1992;**267**:3396–401.
44. Lombardi P, Mulder M, van der Boom H, Frants RR, Havekes LM. Inefficient degradation of triglyceride-rich lipoprotein by HepG2 cells is due to a retarded transport to the lysosomal compartment. *J Biol Chem* 1993;**268**:26113–9.
45. Irie M. Structure-function relationships of acid ribonucleases: lysosomal, vacuolar, and periplasmic enzymes. *Pharmacol Ther* 1999;**81**:77–89.
46. Kielian MC, Marsh M, Helenius A. Kinetics of endosome acidification detected by mutant and wild-type Semliki Forest virus. *EMBO J* 1986;**5**: 3103–9.
47. Hafez IM, Maurer N, Cullis PR. On the mechanism whereby cationic lipids promote intracellular delivery of polynucleic acids. *Gene Ther* 2001;**8**:1188–96.
48. Akinc A, Querbes W, De S, Qin J, Frank-Kamenetsky M, Jayaprakash KN, et al. Targeted delivery of RNAi therapeutics with endogenous and exogenous ligand-based mechanisms. *Mol Ther* 2010;**18**:1357–64.